DOI: 10.1002/ente.201402091

Methanol Synthesis from CO_2 Hydrogenation over CuO–ZnO–TiO_2 Catalysts: The Influence of TiO_2 Content

Jie Xiao, Dongsen Mao,* Xiaoming Guo, and Jun Yu[a]

A series of CuO–ZnO–TiO_2 catalysts with various TiO_2 loadings were prepared by using a co-precipitation method. The prepared catalysts were characterized by using X-ray diffraction (XRD), N_2 adsorption, reactive N_2O adsorption, X-ray photoelectron spectroscopy (XPS), temperature-programmed reduction (TPR), hydrogen temperature programmed desorption (H_2-TPD), and CO_2-TPD techniques, and tested the extent of methanol synthesis from carbon dioxide (CO_2) hydrogenation. The results indicate that the addition of TiO_2 to the CuO–ZnO catalyst makes the copper species exist in an amorphous-like structure or in much smaller crystallites, which promotes the reduction of CuO. Upon increasing the TiO_2 loading, the metallic Cu surface area (S_{Cu}) of the catalyst rises first and then decreases, exhibiting a maximum at a TiO_2 loading of 10%. The results of the catalytic experiments reveal that the addition of TiO_2 favors the production of methanol, and an optimum catalytic activity is obtained at a TiO_2 loading of 10%. Moreover, the methanol yield increases linearly with the S_{Cu} of the catalysts, thereby indicating that the addition of TiO_2 enhances the S_{Cu} but not the intrinsic activity.

Introduction

As a greenhouse gas, CO_2 emissions have been considered as a cause of the environmental problems in the form of the greenhouse effect and ozone depletion. However, CO_2 is a valuable carbon resource that can be converted into fuels and chemicals such as methanol, methane, syngas ($CO+H_2$) and dimethyl ether (DME).[1–5] Up to now, most of the existing research focuses on CO_2 hydrogenation to methanol because methanol is an important feedstock for the organic chemical industry and a potential alternative to fossil fuels.[1–6] Furthermore, an assessment of the economic feasibility for this process supports the possibility.[7] Based on the great potential of methanol synthesis from CO_2 hydrogenation, Olah et al.[2,7,8] proposed a new concept of "methanol economy".

A practical methanol synthesis process requires a high-performance catalyst. Over the past decades, the CuO–ZnO catalyst has been intensively studied for methanol synthesis from CO_2 hydrogenation.[4,5,9] To further enhance the performance of the CuO–ZnO catalyst, numerous promoters and/or supports are added, such as Al,[10,11] Zr,[10] Ga,[12] Cr,[10,11] Y,[12,13] Mg,[13] and Ce.[13,14] Among them, the CuO–ZnO–ZrO_2 catalyst has been investigated most extensively due to its high activity and stability.[15–23] Surprisingly, TiO_2 has received little attention as a promoter or support for the CuO–ZnO catalyst in methanol synthesis from CO_2 although it possesses many similar properties as ZrO_2.[24]

In this work, a systematic study was conducted of the effect of TiO_2 on the CuO–ZnO catalyst for methanol synthesis through CO_2 hydrogenation. The properties of the CuO–ZnO–TiO_2 catalysts were extensively characterized by X-ray diffraction (XRD), N_2 adsorption, reactive N_2O adsorption, X-ray photoelectron spectroscopy (XPS), temperature-programmed reduction (TPR), hydrogen temperature programmed desorption (H_2-TPD), and CO_2-TPD techniques, and the catalytic activity for methanol synthesis from CO_2 hydrogenation was investigated. The main focus of the study is the effect of TiO_2 loading on the physicochemical and catalytic properties of the CuO–ZnO–TiO_2 catalyst.

Results and Discussion

Structural and textural characterizations

In this study, the undoped CuO–ZnO catalyst is denoted as CZ, and the TiO_2 doped CuO–ZnO catalysts are denominated as CZT-x, in which "x" is the molar percentage of TiO_2 relative to the total amount of metallic oxides. As shown in Table 1, the metal compositions of the calcined catalysts are in agreement with the atomic ratios of the starting precursor salts added.

The XRD patterns of CuO–ZnO–TiO_2 catalysts with various TiO_2 loadings are shown in Figure 1. The diffraction peaks at 2θ values of 35.8°, 38.9°, and 49.0° are ascribed to the CuO phase (PDF #48-1548), and those at 32.0°, 34.6°, 36.4°, 47.5°, 56.6°, 62.9°, and 68.0° are ascribed to ZnO phase (PDF #36-1451). Note that the diffraction peaks of CuO and ZnO of the CuO–ZnO catalyst at 2θ values of 35–39° and 47–49° can be distinguished, indicating that the sizes of CuO

[a] J. Xiao, Prof. D. Mao, Dr. X. Guo, Dr. J. Yu
School of Chemical and Environmental Engineering
Shanghai Institute of Technology
100# Haiquan Road, Shanghai 201418 (PR China)
Fax: (+86) 21-6087-3625
E-mail: dsmao@sit.edu.cn

Table 1. Physicochemical properties of the CuO–ZnO and CuO–ZnO–TiO_2 catalysts.

Catalyst	Composition [mol %][a]			S_{BET} [$m^2 g^{-1}$]	Pore volume [$cm^3 g^{-1}$]	Pore size [nm]	S_{Cu} [$m^2 g^{-1}$]	D_{Cu}[b] [%]
	Cu	Zn	Ti					
CZ	49(50)	51(50)	–	30	0.23	29.9	3.09	1.20
CZT-10	44(45)	43(45)	13(10)	69	0.37	21.2	3.84	1.66
CZT-20	34(40)	34(40)	32(20)	123	0.54	17.6	3.66	1.78
CZT-30	30(35)	31(35)	38(30)	140	0.45	12.8	2.92	1.63

[a] Values in parenthesis are nominal fractions of metals. [b] D_{Cu} represents dispersion of Cu and was calculated by exposed copper atoms/total copper atoms.

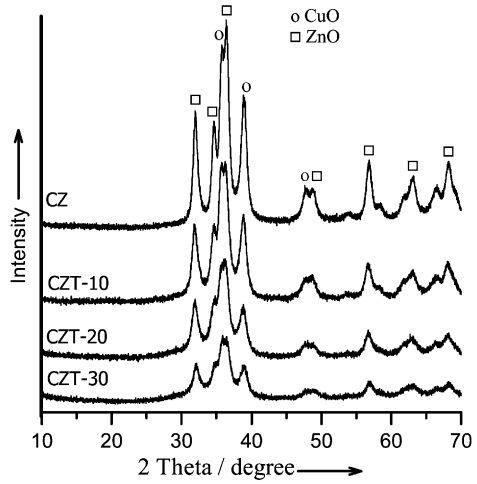

Figure 1. XRD patterns of the CuO–ZnO–TiO_2 catalysts with different TiO_2 loadings.

and ZnO crystallites are relatively large and the interaction of CuO and ZnO is relatively weak. The following effects can been found with the addition of TiO_2:

(1) After the addition of TiO_2 to the CuO–ZnO catalyst, the diffraction peaks for CuO and ZnO weakened evidently and the line width broadened slightly; the effect increased gradually with the increase in the TiO_2 loading. This result indicates that the crystallization degree of CuO and ZnO as well as the sizes of CuO and ZnO crystallites decrease with increasing TiO_2 loading on the CuO–ZnO–TiO_2 catalysts.

(2) The diffraction peaks of CuO and ZnO on the CuO–ZnO–TiO_2 catalysts are superimposed on each other at 2θ values of 35–39° and 47–49°, especially for the samples with high TiO_2 loadings. This result indicates that the addition of TiO_2 enhances the interaction between CuO and ZnO and makes the smaller CuO crystallites disperse in the ZnO crystallites to form a copper–zinc solid solution.[25,26]

It is concluded that the addition of TiO_2 enhances the dispersion of CuO and ZnO in the catalyst body, leading to the higher S_{BET} as shown in Table 1 and the easier reduction of CuO as shown in Figure 3 (H_2-TPR). At the same time, the interdispersion of CuO and ZnO enhances the interaction between CuO and ZnO. This results in positive effects for the catalytic activity of the CuO–ZnO catalyst in methanol synthesis from CO_2 hydrogenation.

On the other hand, as shown in Figure 1, the characteristic peaks of the TiO_2 phase are not observed on the TiO_2-containing samples, indicating that the TiO_2 are amorphous, or well-dispersed as small grains in the catalyst body that cannot be detected using the XRD technique.[27]

As shown in Table 1, in comparison with the CuO–ZnO catalyst, the S_{BET} values of the CuO–ZnO–TiO_2 catalysts increase gradually with increasing TiO_2 loading. The pore sizes of the catalysts are in the reverse order of the Brunauer–Emmett–Teller (BET) surface areas of the catalysts. These results can be attributed to decreases in the size of the CuO and ZnO crystallites in the CuO–ZnO–TiO_2 catalysts, as evidenced by the XRD results (Figure 1). On the other hand, the variation trend of pore volume takes on a volcano shape and a maximum was observed for the CZT-20 catalyst.

S_{Cu} measurement

As shown in Table 1, the S_{Cu} values of the reduced Cu–ZnO–TiO_2 catalysts increase first and then decrease with increasing the content of TiO_2 between 0 and 30%. This change can be explained as follows: on one hand, the doping of TiO_2 can enhance the dispersion of CuO (as shown in Figure 1) and can be verified by the increase in the D_{Cu} from CZ to CZT-20 as shown in Table 1, which results in the enlargement of S_{Cu}. On the other hand, the increase in TiO_2 loading will lead to a decrease in Cu content in the catalyst because the ratio of Cu/Zn remains constant. The decrease in Cu content in the catalyst will inevitably have a negative effect on S_{Cu}. For TiO_2 loading amounts of less than 10%, the former is a predominant factor. On the contrary, the latter prevails over the former if the loading amount is more than 10%. Furthermore, the Cu surface sites will be occupied partially by TiO_2[24] and this was confirmed by the fact that the D_{Cu} on the CTZ-30 catalyst was lower than that on the CTZ-20 catalyst. The result of the combined effect of these factors is that a maximum of S_{Cu} is obtained with a TiO_2 loading of 10%.

XPS analysis

Figure 2 shows XPS patterns of the Cu2p, Zn2p, and Ti2p regions for the two representative CZ and CZT-10 catalysts. The binding energies (BEs) of Cu$2p_{3/2}$ and Zn$3d_{3/2}$ core electrons are summarized in Table 2. According to the literature,[28] the binding energy of the Cu$2p_{3/2}$ peak at approximately 933 eV together with the characteristic shake-up feature at 942 eV are indicative of Cu^{2+} species, which further indicates that copper species are present as Cu^{2+} in both CZ and CZT-10 catalysts. With the addition of TiO_2, there are no significant variations in the binding energies of Cu$2p_{3/2}$, indicating that the chemical state of CuO was not influenced noticeably by the addition of TiO_2. Furthermore, as shown in Table 2, there are no variations in the binding energy of Zn$2p_{3/2}$ with TiO_2 doping, indicating that the addition of

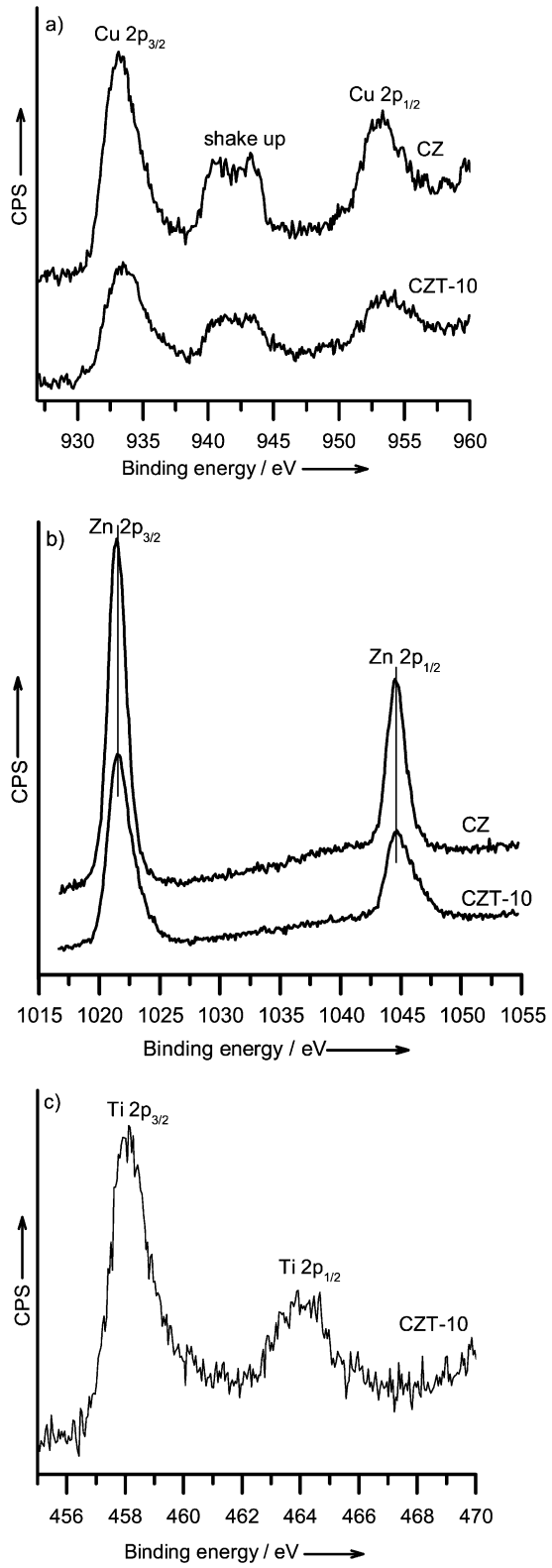

Figure 2. XPS spectra of Cu 2p (a), Zn 2p (b), and Ti 2p (c) for the CZ and CZT-10 catalysts.

TiO_2 has no evident effect on the chemical state of Zn either. Figure 2c shows that the binding energies of $Ti\,2p_{3/2}$ and $Ti\,2p_{1/2}$ are centered at 458.5 eV and 464.1 eV, respectively, which is in good agreement with the reported values for Ti^{4+} in anatase TiO_2.[24]

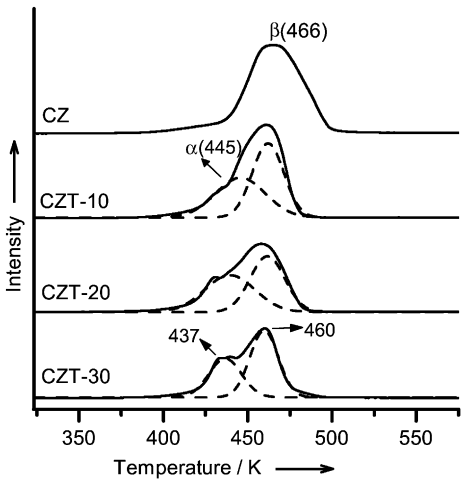

Figure 3. H_2-TPR profiles of the CuO–ZnO–TiO_2 catalysts with different TiO_2 loadings.

Surface compositions of the two catalysts determined using XPS are listed in Table 2. Compared with the average compositions in the bulk catalysts (as shown in Table 2), the surfaces of the catalysts are considerably depleted of Cu. In contrast, an enrichment of Zn on the surface is observed. Similar results were also reported by some researchers on other CuO-based catalysts.[19,29] Moreover, the Cu/Zn ratios of the catalysts are also included in Table 2. Clearly, the Cu/Zn ratios of the two catalysts are almost the same (as shown in Table 2), indicating that the addition of TiO_2 has no noticeable effect on the surface composition of the CuO–ZnO catalyst.

H_2-TPR analysis

To investigate the reduction behavior of the catalysts, TPR measurements were performed and the results are shown in Figure 3. It was observed that the CuO–ZnO catalyst exhibits a broad reduction peak, whereas the CuO–ZnO–TiO_2 catalysts exhibit two reduction peaks in the temperature between 375 and 525 K. As is well documented, the low-temperature peak (α peak) is attributed to the reduction of small particles and highly dispersed CuO surface species, whereas the peak appearing at higher temperature (β peak) is related to the reduction of bulk-like CuO.[30] The shift of position of the β peaks from 466 to 460 K indicated that the particle size of the bulk CuO became smaller from CZ to CZZ-30, because, the greater ease reduction results in smaller particles of CuO.[30] This result is in good agreement with that obtained by XRD measurements (Figure 1). Moreover, the position of the α peaks shifted from 445 to 437 K, indicating that the size of the fine CuO particles also became smaller from CZ-10 to CZZ-30. As expected, the reduction peak areas of the CuO–ZnO–TiO_2 catalysts decrease with increasing TiO_2 content due to the decrease of the amount of CuO in the catalysts.

Table 2. XPS results for the CuO–ZnO and CuO–ZnO–TiO_2 catalysts.

Catalyst	Binding energy [eV]		Relative surface concentration of metal[a] [mol %]			Cu/Zn molar ratio[b]
	Cu $2p_{3/2}$	Zn $2p_{3/2}$	Cu	Zn	Ti	
CZ	933.1	1021.7	39(50)	61(50)	0(0)	0.64(0.96)
CZT-10	933.4	1021.7	33(45)	57(45)	10(10)	0.58(1.02)

[a] Values in parenthesis are nominal fractions of metals. [b] Values in parenthesis were determined by using atomic absorption spectroscopy (AAS).

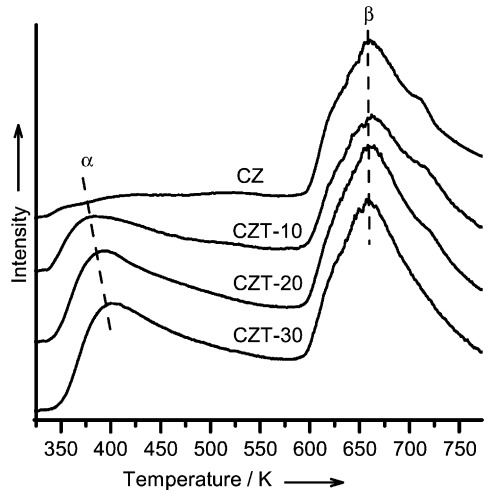

Figure 4. H_2-TPD profiles of the pre-reduced Cu–ZnO–TiO_2 catalysts with different TiO_2 loadings.

H_2-TPD analysis

The H_2-TPD profiles for the pre-reduced catalysts are presented in Figure 4. As seen, all the patterns span a wide range of temperature (323–773 K). Two desorption peaks can be observed for all of the investigated catalysts, which is diagnostic of different adsorption states of hydrogen species across the catalyst structure. According to literature data, only the resolved peak at low temperature is ascribable to atomic hydrogen on surface Cu sites,[31,32] whereas the large signal at high temperature monitors the desorption of hydrogen from either the bulk of Cu particles[31] or from the ZnO surface.[32] The maximum desorption temperature and quantitative data are listed in Table 3. As noted, with the addition of TiO_2, the α peak shifted to higher temperatures slightly (from 384 K to 402 K) and the corresponding peak area increased with increasing TiO_2 content, whereas the β peak had no evident changes. This result indicates that the addition of TiO_2 improves the adsorption of molecular H_2 and dissociates to atomic hydrogen, which can be ascribed to the enhancement in the dispersion of CuO (XRD and H_2-TPR) and enlargement of the S_{Cu} (Table 1). The better adsorption strength of molecular H_2 and the dissociated atomic hydrogen are beneficial to the hydrogenation of activated CO_2 species to form methanol.[33] On the other hand, it should be emphasized that only the H_2 desorbed at lower temperature is useful for the synthesis of methanol from CO_2 hydrogenation as the reaction usually takes place below 623 K.[13] This inference was confirmed by the catalytic activity of different catalysts as described below.

Table 3. Temperatures of desorption peaks and their contributions to H_2-TPD pattern over the pre-reduced catalysts.

Catalyst	T_α [K]	T_β [K]	A_α	A_β
CZ	–	658	41	285
CZT-10	384	658	109	272
CZT-20	392	658	168	277
CZT-30	402	658	190	296

CO_2-TPD analysis

Figure 5 shows the CO_2-TPD curves of the pre-reduced Cu–ZnO–TiO_2 catalysts with different TiO_2 contents. Two desorption peaks (denoted as α and β, respectively) are observed in lower and higher temperature ranges, corresponding to a weak basic site and a strong basic site, respectively. The maximum desorption temperature and quantitative data are listed in Table 4. As can be noted, the shift of the α peak from 425 to 415 K indicates that the weak basic site becomes weaker as the TiO_2 loading increases from 0 to 30 %; whereas the temperature of the β peak exhibited no noticeable change. On the other hand, the intensities of both the α peak and β peak over the Cu–ZnO–TiO_2 catalysts are larger than those over the Cu–ZnO catalyst, indicating that the addition of TiO_2 increases the amounts of CO_2 adsorbed on both weak and strong basic sites. In other words, the addition of TiO_2 enhances the basicity on the surface of the Cu–ZnO catalyst, which is beneficial to the adsorption of acidic CO_2 and ultimately increases the activity.[34] Based on the peak in-

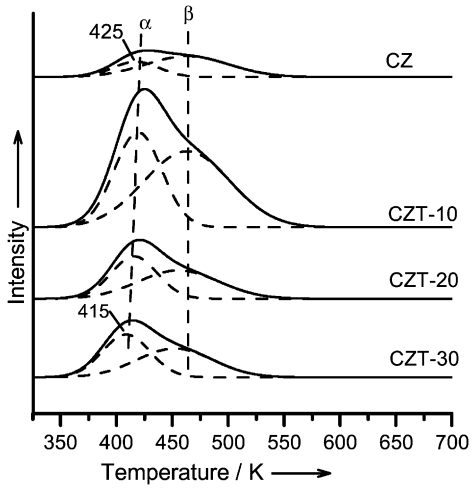

Figure 5. CO_2-TPD profiles of pre-reduced Cu–ZnO–TiO_2 catalysts with different TiO_2 loadings.

Table 4. Temperatures of the desorption peaks and their contributions to the CO_2-TPD pattern over the pre-reduced catalysts.

Catalyst	T_α [K]	T_β [K]	A_α (a.u.)	A_β (a.u.)
CZ	425	464	51	127
CZT-10	425	464	336	488
CZT-20	420	462	145	170
CZT-30	415	462	152	164

tensity of the four catalysts, the activity would increase in the order of CZ < CZT-30 < CZT-20 < CZT-10. This speculation was verified by the reaction results described below.

Catalytic performance

Activity and selectivity measurement results for methanol synthesis from CO_2 hydrogenation over the reduced Cu–ZnO–TiO_2 catalysts with various TiO_2 loadings are summarized in Figure 6. Methanol and CO are the only carbon-containing products under the present reaction conditions and traces of methane can be detected at high temperatures. The effect of reaction temperature on the catalytic performance of the Cu–ZnO–TiO_2 catalysts with different TiO_2 loadings was investigated and the results are presented in Figure 6. As observed for all of the catalysts, the conversion of CO_2 increased with increasing reaction temperature (Figure 6a), accompanied by a decrease in methanol selectivity (Figure 6b) over the temperature range of 473–553 K. The variation of methanol yield with reaction temperature is presented in Figure 6c. Clearly, a maximum yield of methanol, which represents the critical point of the reaction transforming from a kinetically limited regime to a thermodynamically defined one, exists for all the catalysts studied.[35] Furthermore, it is clear that the addition of TiO_2 is favorable for the production of methanol and the sample of CZT-10 shows the highest methanol yield, as shown in Figure 6c. On the other hand, the optimum reaction temperature is at 506 K over the Cu–ZnO–TiO_2 catalysts, which is lower than that (516 K) of the TiO_2-free Cu–ZnO catalyst. This is an important advantage for the methanol synthesis catalyst because methanol synthesis is an extremely exothermic reaction.

It is worth noting that the difference in the CO_2 conversion between CZ and CZT catalysts decreases with increasing reaction temperature (Figure 6a) because the CO_2 conversion is approaching the equilibrium conversion. Therefore, the activity comparison between the different catalysts would be meaningful at low reaction temperatures. From this point of view, the CO_2 conversion, methanol selectivity, and space-time yield (STY) of methanol over the Cu–ZnO–TiO_2 catalysts are plotted against their TiO_2 contents at 493 K and presented in Figure 7.

As shown in Figure 7a, the conversion of CO_2 increases with the addition of TiO_2 and a maximum of 14.8% is observed over the sample of CZT-10. In comparison with the TiO_2-free Cu–ZnO, this value increases by 14%. Further addition of TiO_2 leads to a decrease in CO_2 conversion. This

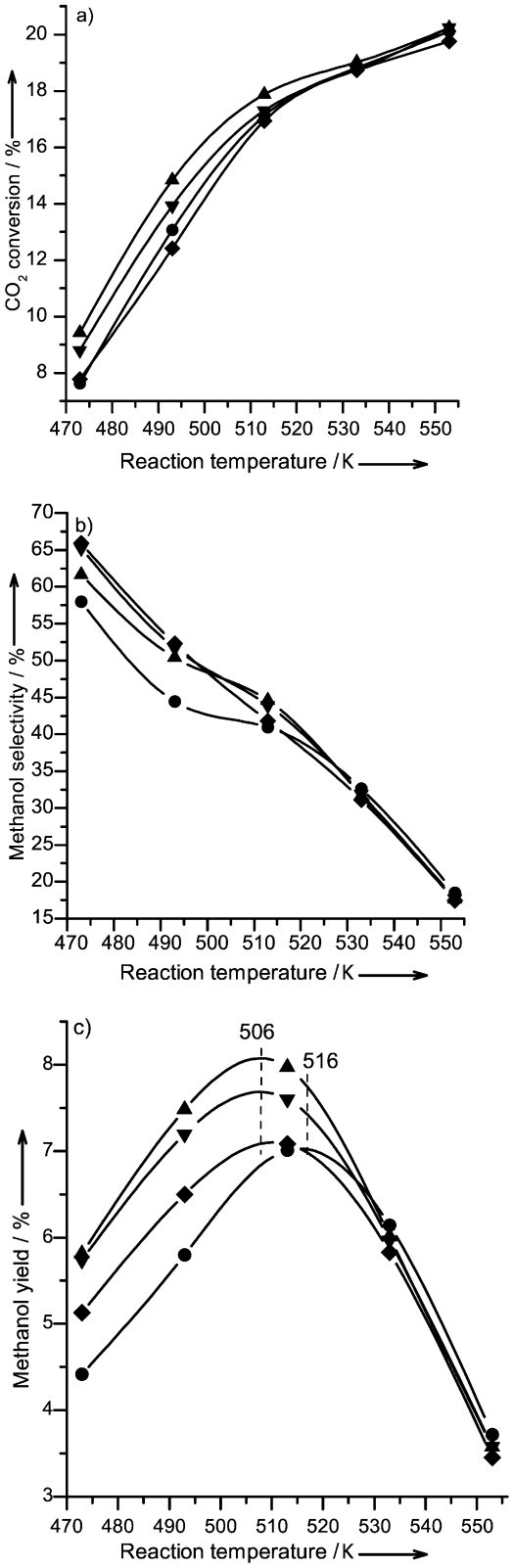

Figure 6. Effect of reaction temperature on catalytic performance of the Cu–ZnO–TiO_2 catalyst. (a) CO_2 conversion, (b) Methanol selectivity, (c) Methanol yield. ●: CZ; ▲: CZT-10; ▼: CZT-20; ■: CZT-30. Reaction conditions: $H_2/CO_2 = 3$, $P = 3.0$ MPa, GHSV = 2400 h^{-1}.

result is in disagreement with that reported by Arakawa et al.[24] who found that the addition of TiO_2 with a content

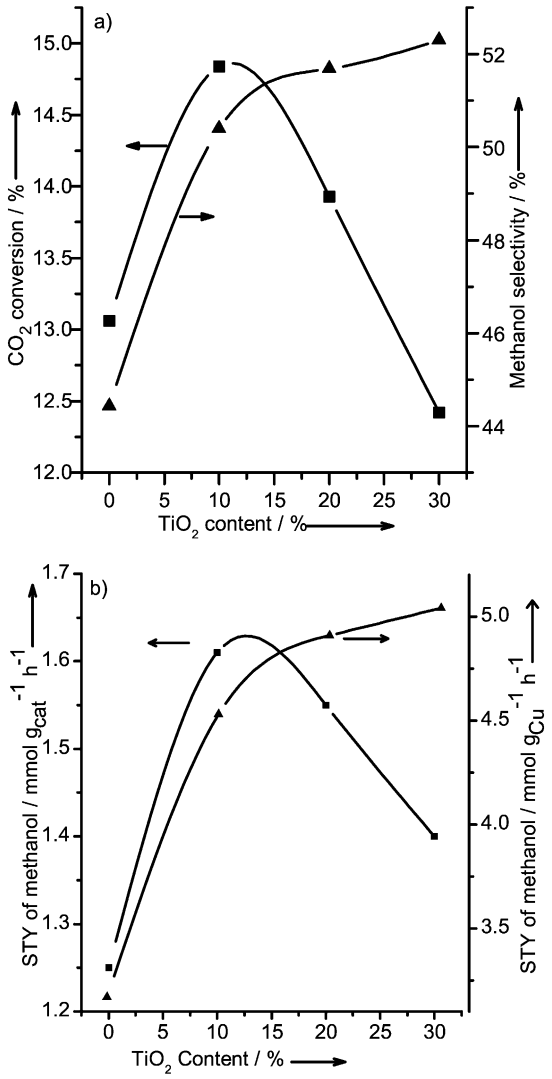

Figure 7. Effect of TiO_2 content on catalytic performance of the Cu-ZnO-TiO_2 catalyst. (a) CO_2 conversion and methanol selectivity; (b) Space-time yield of methanol. Reaction conditions: $T=493$ K, $H_2/CO_2=3$, $P=3.0$ MPa, GHSV $=2400\ h^{-1}$.

of 35% slightly increased the CO_2 conversion. On the other hand, the selectivity for CH_3OH is enhanced after the addition of TiO_2 and this continues with increasing TiO_2 content over the Cu–ZnO–TiO_2 catalysts. The highest value of CH_3OH selectivity (52.3%) is observed over the CZT-30 catalyst, which is 18% higher than that on the undoped Cu–ZnO catalyst. On the other hand, as shown in Figure 7b, the highest STY of CH_3OH is obtained over the CZT-10 catalyst, and the value increased by approximately 30% (from 1.25 to 1.61 mmol $g_{cat}^{-1}h^{-1}$) in comparison with the TiO_2-free Cu–ZnO catalyst. Considering the different Cu contents in the various catalysts (Table 1), the specific methanol synthesis activities (i.e., STY of CH_3OH per gram Cu) of the various catalysts was also calculated; the results are also presented in Figure 7b. It was observed that the specific methanol synthesis activity increased continuously with increased TiO_2 content, indicating that the efficiency of the utilization of the active Cu species increased continuously with increasing TiO_2 content. The results described above suggest that the amount of TiO_2 has a remarkable influence on the catalytic performance of the Cu–ZnO–TiO_2 catalysts.

It has been well known that S_{Cu} is an important parameter for methanol synthesis from CO_2 hydrogenation over the Cu-based catalysts. The relationship between the S_{Cu} and catalytic activity for this reaction over Cu-based catalysts has been studied extensively, though some controversies still remain. For example, Sloczynski,[19] Chinchen et al.,[36,37] and Witoon et al.[38] reported that there was a linear relationship between the methanol yield of such catalysts and their copper surface areas. However, Arena et al.[17] and Sun et al.[35] point out that the methanol yield increased with increasing S_{Cu}, but it was not a linear relationship. In our experiment, the effect of the surface area of metallic copper on the activity of methanol synthesis through CO_2 hydrogenation over the Cu–ZnO–TiO_2 catalysts with different TiO_2 loadings was studied, and the result is presented in Figure 8. It is observed that the catalytic activity increases linearly with increasing S_{Cu}, indicating that TiO_2 improves the dispersion of Cu particles without changing the intrinsic activity of the CuO–ZnO catalyst. This conclusion was also supported by the results obtained through XPS characterization that the addition of TiO_2 had no noticeable effect on the chemical state of the Cu and Zn species as well as the surface composition of the CuO–ZnO catalyst (Table 2). This result is in contrast to that reported by Arakawa et al.[24] who found that the addition of TiO_2 increased the TOF for methanol formation whereas the S_{Cu} decreased significantly. The discrepancy may be caused by the different metallic salts and conditions used for the preparation of the catalysts. The effect of TiO_2 observed in our study is the same as that of ZrO_2 or Al_2O_3 on the CuO–ZnO catalyst,[10] that is, the TiO_2 in the catalyst plays a structural promoter role.

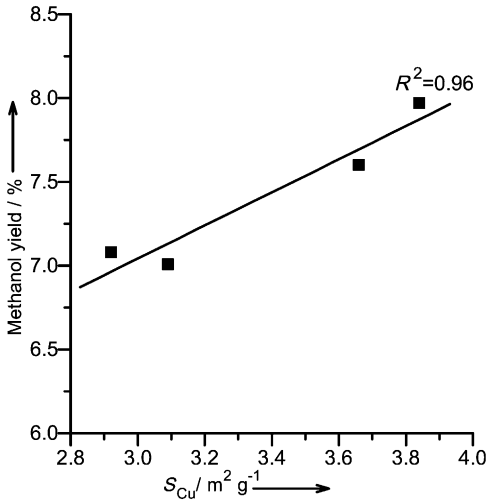

Figure 8. The relationship between methanol yield and the surface area of metallic copper (S_{Cu}).

Conclusions

Cu–ZnO–TiO_2 catalysts with various TiO_2 loadings were prepared using co-precipitation for methanol synthesis by CO_2 hydrogenation. The influences of TiO_2 loadings on the physicochemical and catalytic properties of the Cu–ZnO–TiO_2 catalysts were investigated. Based on the results of this study, the following conclusions can be made:

(1) The addition of TiO_2 leads to a decrease in crystallite sizes of catalysts and makes copper in the catalyst exhibit amorphous-like or less-well-ordered structural features and enhances the synergetic effect between CuO and ZnO.

(2) With the increase in TiO_2 loading, the metallic copper surface area (S_{Cu}) and the number of basic sites take on a volcano-shaped variation trend and the amount of H_2 adsorption increases monotonically over the Cu–ZnO–TiO_2 catalysts.

(3) The methanol yield depends on the surface area of metallic copper, and a linear relationship exists between them.

(4) The optimum reaction temperature of the Cu–ZnO–TiO_2 catalyst is lower than that of the Cu–ZnO catalyst.

(5) A suitable amount of TiO_2 is beneficial for the catalytic activity of Cu–ZnO–TiO_2 for methanol synthesis from CO_2 hydrogenation, and a maximum methanol yield is obtained at the TiO_2 loading of 10%.

Experimental Section

Catalyst preparation

A series of CuO–ZnO–TiO_2 catalysts with various TiO_2 loadings were prepared by using carbonate co-precipitation, in which the CuO and ZnO molar ratio was maintained at 1:1, and the molar percentage of TiO_2 ranged from 0 to 30% relative to the total amount of metallic oxides. All chemicals used in this work were of reagent grade purity (Shanghai Chemical Reagent Corporation, China). Firstly, the required amounts of metallic salts [$Cu(NO_3)_2{\cdot}3H_2O$, $Zn(NO_3)_2{\cdot}6H_2O$, $Ti(SO_4)_2$] were dissolved in deionized water to form a solution. Then the two aqueous solutions of metallic salts and sodium carbonate (0.8 M) were added slowly and simultaneously into 50 mL of deionized water under vigorous stirring. The pH was kept constant at 9.0–10.0. The precipitates were kept in an ultrasound bath operating at 47 kHz with a power of 30 W for 0.5 h. Afterwards, the precipitates were aged at 363 K for 3 h, then filtered, thoroughly washed with 343 K hot deionized water, and dried at 383 K overnight. The dried samples were ground into a fine powder and were calcined in air at 673 K (ramp rate = 2 K min^{-1}) for 4 h. In this study, the undoped CuO–ZnO catalyst is denoted as CZ, and the TiO_2 doped CuO–ZnO catalysts are denominated as CZT-*x*, in which "*x*" is the molar percentage of TiO_2 relative to the total amount of metallic oxides.

Catalyst characterization

Full nitrogen adsorption/desorption isotherms at 77 K were obtained after outgassing the sample under vacuum at 473 K for 10 h using a Micromeritics ASAP2020 M + C adsorption apparatus. The BET specific surface area (S_{BET}) was calculated using a value of 0.162 nm^2 for the cross-sectional area of the nitrogen molecule. Pore size distributions were determined by the Barrett–Joyner–Halenda (BJH) method using the equation of Halsey.

X-ray diffraction (XRD) patterns were recorded using a PANalytical X'Pert diffractometer operating with Ni β-filtered $Cu_{K\alpha}$ radiation at 40 KV and 40 mA. Two-theta angles ranged from 10° to 70° with a speed of 6° per minute.

Cu and Zn contents of the calcined catalysts were determined by atomic absorption spectroscopy (AAS) on acid-digested samples, using a SpectrAA-220 atomic absorption spectrometer (VARIAN).

The metallic copper surface areas (S_{Cu}) of the reduced catalysts were determined using a N_2O chemisorption method.[15] Once the catalyst was reduced in a 10% H_2/N_2 mixture at 573 K for 1 h, it was exposed to a flow of He and cooled to the chemisorption temperature (333 K). Then, a flow of 2 vol% N_2O/He gas mixture was fed into the reactor. The N_2 produced by the decomposition of N_2O on the exposed Cu atoms was detected using a mass spectrometer (Pefeiffer Vacuum Quadstar, 32-bit). The metallic copper surface density of 1.46×10^{19} Cu atoms m^{-2} and a molar stoichiometry of $N_2O/Cu = 0.5$ were used to calculate the S_{Cu}.[20]

X-ray photoelectron spectroscopy (XPS) measurements were performed using a Kratos Axis Ultra DLD spectrometer equipped with an $Al_{K\alpha}$ (1486.6 eV) X-ray exciting source. The pass energy of the analyzer was set 40 eV. The banding energies were referenced to the adventitious C 1s peak at 284.6 eV (accuracy within ±0.3 eV).

Temperature-programmed reduction (TPR) measurements were performed using a continuous-flow apparatus fed with a 10% H_2/N_2 mixture flowing at 30 mL min^{-1} and heated at a rate of 5 K min^{-1} to 573 K. Approximately 0.1 g of catalyst was used, and the H_2 consumption was monitored using a thermal conductivity detector (TCD).

Hydrogen temperature programmed desorption (H_2-TPD) was performed in a quartz tubular reactor. Firstly, the catalyst sample was reduced at 573 K for 1 h in flowing 10% H_2/N_2 mixture. Then the sample was cooled to 323 K and further saturated in H_2/N_2 mixture for 0.5 h, followed by flushing in N_2 for 1 h. The TPD measurements were conducted in a N_2 stream (30 mL min^{-1}) from 323 K to 773 K at a heating rate of 5 K min^{-1}. The change of hydrogen signal was monitored by using a TCD.

The basicity of the catalyst was measured by CO_2 temperature-programmed desorption (CO_2-TPD). Prior to the adsorption of CO_2, the catalysts were reduced at 573 K for 1 h in flowing 10% H_2/N_2 gas mixture. Then the sample was cooled to 323 K and further saturated in a 10% CO_2/N_2 (30 mL min^{-1}) mixture for 0.5 h, followed by flushing in He for 1 h to remove any physisorbed molecules. Afterwards, the TPD experiment was started with a heating rate of 10 K min^{-1} under He flow (30 mL min^{-1}), and the desorbed CO_2 was monitored by using a mass spectrometer (Pefeiffer Vacuum Quadstar, 32-bit).

Catalytic activity testing

Activity and selectivity measurements for the CO_2 hydrogenation were performed in a continuous-flow, fixed-bed reactor. The catalyst (≈0.5 g) diluted with quartz sand (both in 40–60 mesh) was packed into the stainless-steel tubular reactor (5 mm i.d.). Preliminary experiments with respect to possible influence of interparticle mass-transfer limitations confirmed that such a limitation

could be ruled out under the conditions used in the present study. Prior to the catalytic measurements, the fresh catalyst was reduced in a stream of 10% H_2/N_2 flowing at 30 mL min^{-1} at 573 K for 3 h under atmospheric pressure. Then the reactor was cooled to a given temperature and a gas mixture ($CO_2/H_2/N_2$ = 22:66:12, molar ratio) with a GHSV (gas hourly space velocity) of 2400 mL h^{-1} g^{-1} was introduced, raising the pressure to 3.0 MPa. All post reactor lines and valves were heated to 443 K to prevent possible product condensation. Effluent products were analyzed on-line using a gas chromatograph (6820, Agilent). The methanol production was determined using a Porapak Q column, a flame-ionization detector (FID); a Carbosieve column and TCD were used for other gaseous products. Conversion and selectivity values were calculated by mass balance, and the steady-state values were quoted as the average of seven different analyses taken after 4 h of on-stream operation.

Acknowledgements

The authors thank the Shanghai Municipal Education Commission (13YZ117) and Science and Technology Commission of Shanghai Municipality (13ZR1441200) for financial support.

Keywords: carbon dioxide · copper · heterogeneous catalysis · methanol synthesis · titanium dioxide

[1] L. Barbato, G. Centi, G. Iaquaniello, A. Mangiapane, S. Perathoner, *Energy Technol.* **2014**, *2*, 453–461.
[2] G. A. Olah, A. Goeppert, G. K. S. Prakash, *J. Org. Chem.* **2009**, *74*, 487–498.
[3] W. Wang, S. Wang, X. Ma, J. Gong, *Chem. Soc. Rev.* **2011**, *40*, 3703–3727.
[4] N. A. M. Razali, K. T. Lee, S. Bhatia, A. R. Mohamed, *Renewable Sustainable Energy Rev.* **2012**, *16*, 4951–4964.
[5] S. Saeidi, N. A. S. Amin, M. R. Rahimpour, *J. CO_2 Util.* **2014**, *5*, 66–81.
[6] R. Raudaskoski, E. Turpeinen, R. Lenkkeri, E. Pongrácz, R. Keiski, *Catal. Today* **2009**, *144*, 318–323.
[7] G. A. Olah, *Angew. Chem. Int. Ed.* **2005**, *44*, 2636–2639; *Angew. Chem.* **2005**, *117*, 2692–2696.
[8] G. A. Olah, *Angew. Chem. Int. Ed.* **2013**, *52*, 104–107; *Angew. Chem.* **2013**, *125*, 112–116.
[9] X. M. Guo, D. S. Mao, G. Z. Lu, S. Wang, *Chem. Ind. Eng. Prog.* **2012**, *31*, 477–488.
[10] M. Saito, T. Fujitani, M. Takeuchi, T. Watanabe, *Appl. Catal. A* **1996**, *138*, 311–318.
[11] M. Saito, M. Takeuchi, T. Watanabe, J. Toyir, S. Luo, J. Wu, *Energy Convers. Manage.* **1997**, *38*, S403–S408.
[12] S. Natesakhawat, J. W. Lekse, J. P. Baltrus, P. R. Ohodnicki, Jr., B. H. Howard, X. Y. Deng, C. Matranga, *ACS Catal.* **2012**, *2*, 1667–1676.
[13] H. Zhan, F. Li, P. Gao, N. Zhao, F. Xiao, W. Wei, L. Zhong, Y. Sun, *J. Power Sources* **2014**, *251*, 113–121.
[14] F. Arena, G. Mezzatesta, G. Zafarana, G. Trunfio, F. Frusteri, L. Spadaro, *J. Catal.* **2013**, *300*, 141–151.
[15] X. M. Guo, D. S. Mao, G. Z. Lu, S. Wang, G. S. Wu, *J. Catal.* **2010**, *271*, 178–185.
[16] X. M. Guo, D. S. Mao, G. Z. Lu, S. Wang, G. S. Wu, *Catal. Commun.* **2011**, *12*, 1095–1098.
[17] J. Słoczyński, R. Grabowski, A. Kozłowska, P. Olszewski, J. Skrzypek, M. Lachowska, J. Skrzypek, J. Stoch, *Appl. Catal. A* **2003**, *249*, 129–138.
[18] J. Słoczyński, R. Grabowski, A. Kozłowska, P. Olszewski, J. Stoch, J. Skrzypek, M. Lachowska, *Appl. Catal. A* **2004**, *278*, 11–23.
[19] J. Sloczynski, R. Grabowski, P. Olszewski, A. Kozlowska, J. Stoch, M. Lachowska, J. Skrzypek, *Appl. Catal. A* **2006**, *310*, 127–137.
[20] F. Arena, G. Italiano, K. Barbera, S. Bordiga, G. Bonura, L. Spadaro, F. Frusteri, *Appl. Catal. A* **2008**, *350*, 16–23.
[21] F. Arena, K. Barbera, G. Italiano, G. Bonura, L. Spadaro, F. Frusteri, *J. Catal.* **2007**, *249*, 185–194.
[22] G. Bonura, M. Cordaro, C. Cannilla, F. Arena, F. Frusteri, *Appl. Catal. B* **2014**, *152–153*, 152–161.
[23] R. Ladera, F. J. Perez-Alonso, J. M. Gonzalez-Carballo, M. Ojeda, S. Rojas, J. L. G. Fierro, *Appl. Catal. B* **2013**, *142–143*, 241–248.
[24] H. Arakawa, K. Sayama, K. Okabe, A. Murakami, *Stud. Surf. Sci. Catal.* **1993**, *77*, 389–392.
[25] M. Spencer, *Catal. Lett.* **2000**, *66*, 255–257.
[26] X. J. Guo, L. M. Li, S. M. Liu, G. L. Bao, W. H. Hou, *J. Fuel Chem. Technol.* **2007**, *35*, 329–333.
[27] T. J. Hu, H. B. Yin, R. C. Zhang, H. X. Wu, T. S. Jiang, Y. Wada, *Catal. Commun.* **2007**, *8*, 193–199.
[28] B. R. Bechara, A. Aboukai's, J. P. Bonnelle, *J. Chem. Soc. Faraday Trans.* **1993**, *89*, 1257–1262.
[29] M. Kilo, J. Weigel, A. Wokaun, R. A. Koeppel, A. Stoeckli, A. Baiker, *J. Mol. Catal. A* **1997**, *126*, 169–184.
[30] Y. Zhang, J. Fei, Y. Yu, X. Zheng, *Energy Convers. Manage.* **2006**, *47*, 3360–3367.
[31] H. Wilmer, T. Genger, O. Hinrichsen, *J. Catal.* **2003**, *215*, 188–198.
[32] P. Gao, F. Li, L. N. Zhang, N. Zhao, F. K. Xiao, W. Wei, L. S. Zhong, Y. H. Sun, *J. CO_2 Util.* **2013**, *2*, 16–23.
[33] L. X. Zhang, Y. C. Zhang, S. Y. Chen, *Appl. Catal. A* **2012**, *415–416*, 118–123.
[34] T. Inui, T. Takeguchi, A. Kohama, K. Tanida, *Energy Convers. Manage.* **1992**, *33*, 513–520.
[35] Q. Sun, Y. L. Zhang, H. Y. Chen, J. F. Deng, D. Wu, S. Y. Chen, *J. Catal.* **1997**, *167*, 92–105.
[36] G. C. Chinchen, K. C. Waugh, D. A. Whan, *Appl. Catal.* **1986**, *25*, 101–107.
[37] G. C. Chinchen, P. J. Denny, D. G. Parker, M. S. Spencer, D. A. Whan, *Appl. Catal.* **1987**, *30*, 333–338.
[38] T. Witoon, T. Permsirivanich, W. Donphai, A. Jaree, M. Chareonpanich, *Fuel Process. Technol.* **2013**, *116*, 72–78.

Received: August 7, 2014
Published online on October 15, 2014

